PTFE Tribology and the Role of Mechanochemistry in the Development of Protective Surface Films

ARTICLE *in* MACROMOLECULES · MAY 2015

Impact Factor: 5.8 · DOI: 10.1021/acs.macromol.5b00452

7 AUTHORS, INCLUDING:

W. Gregory Sawyer
University of Florida
205 PUBLICATIONS **3,844** CITATIONS
SEE PROFILE

Brandon Krick
Lehigh University
31 PUBLICATIONS **240** CITATIONS
SEE PROFILE

Macromolecules

Article

pubs.acs.org/Macromolecules

PTFE Tribology and the Role of Mechanochemistry in the Development of Protective Surface Films

Kathryn L. Harris,[†] Angela A. Pitenis,[‡] W. Gregory Sawyer,[†,‡] Brandon A. Krick,[§] Gregory S. Blackman,[∥] Daniel J. Kasprzak,[∥] and Christopher P. Junk*[,∥]

[†]Department of Materials Science and Engineering and [‡]Department of Mechanical and Aerospace Engineering, University of Florida, Gainesville, Florida 32611, United States

[§]Department of Mechanical Engineering and Mechanics Lehigh University, Bethlehem, Pennsylvania 18015, United States

[∥]Experimental Station E500/2604B, DuPont Central Research and Development, 200 Powder Mill Road, P.O. Box 8352 Wilmington, Delaware 19803, United States

ABSTRACT: The wear and friction behavior of ultralow wear polytetrafluoroethylene (PTFE)/α-alumina composites first described by Burris and Sawyer in 2006 has been heavily studied, but the mechanisms responsible for the 4 orders of magnitude improvement in wear over unfilled PTFE are still not fully understood. It has been shown that the formation of a polymeric transfer film is crucial to achieving ultralow wear on a metal countersurface. However, the detailed chemical mechanism of transfer film formation and its role in the exceptional wear performance has yet to be described. There has been much debate about the role of chemical interactions between the PTFE, the filler, and the metal countersurface, and some researchers have even concluded that chemical changes are *not* an important part of the ultralow wear mechanism in these materials. Here, a "stripe" test allowed detailed spectroscopic studies of PTFE/α-alumina transfer films in various stages of development, which led to a proposed mechanism which accounts for the creation of chemically distinct films formed on both surfaces of the wear couple. PTFE chains are broken during sliding and undergo a series of reactions to produce carboxylate chain ends, which have been shown to chelate to both the metal surface and to the surface of the alumina filler particles. These tribochemical reactions form a robust polymer-on-polymer system that protects the steel countersurface and is able to withstand hundreds of thousands of cycles of sliding with almost no wear of the polymer composite after the initial run-in period. The mechanical scission of carbon−carbon bonds in the backbone of PTFE under conditions of sliding contact is supported mathematically using the Hamaker model for van der Waals interactions between polymer fibrils and the countersurface. The necessity for ambient moisture and oxygen is explained, and model experiments using small molecules confirm the reactions in the proposed mechanism.

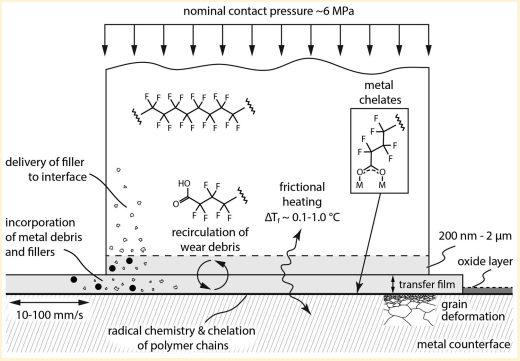

1. INTRODUCTION

Surface interfaces are the least understood and by extension perhaps the most critical design element in machines and mechanical assemblies. Tribological phenomena (*i.e.* friction and wear) at these interfaces are fundamental to system performance, longevity, and reliability. The two most common metrics for tribological interactions are friction coefficient and wear rate. Contrary to rudimentary intuition, they are not material properties and low friction does not equal low wear. Instead, they are a function of numerous system parameters, including material pairing, applied contact pressure, sliding velocity, sliding geometry and environmental conditions. Furthermore, these metrics are temporally variant and depend on a series of seemingly rare interactions that are a function of multiscale mechanics, chemistry, physics and materials phenomena.

Solid lubricants are of immense tribological importance at these interfaces because of the breadth of applications in which they are more desirable than other engineering materials due to higher operating temperatures and contact pressures, vacuum environments, or reciprocating motions. Polytetrafluoroethylene (PTFE) in particular is used in a large number of tribological applications because of its uniquely low coefficient of friction.[1−5] However, the neat polymer has very poor wear characteristics ($K \sim 7 \times 10^{-4}$ mm^3/(N·m)).[5−9] PTFE composites have been widely studied because the inclusion of fillers improved the wear rate by 1−2 orders of magnitude.[6−8,10−12] Wear abatement of PTFE using fillers of various sizes and chemical composition is mechanistically unique, as PTFE itself has been shown to wear in a manner quite contrary to other engineering polymers and the mechanism thereof has been of interest for decades.[5,6,13−15]

The inclusion of micrometer-sized metal oxide particles (ZrO_2 and TiO_2) reduced the wear rate of PTFE by 1 or 2

Received: March 3, 2015
Revised: May 7, 2015

DOI: 10.1021/acs.macromol.5b00452
Macromolecules XXXX, XXX, XXX−XXX

orders of magnitude, and was initially favored over the inclusion of nanoparticles which were thought too small to prevent excessive wear of the polymer.[9] At the time, wear reduction via fillers was considered from a largely mechanical standpoint. In the 1990s and 2000s, certain nanoparticles were shown to be relatively effective at reducing the wear rate of PTFE,[7,16] in 2002 Li experimented with reducing wear using various loadings of ZnO nanoparticles,[17] and in 2006 Burris and Sawyer discovered that five weight percent α-phase alumina particles reduced wear by an additional factor of 100, a total of 4 orders of magnitude improvement compared to the neat PTFE.[18] The term "ultralow wear" PTFE composites has been used to describe several exceptional materials with wear rates less than 10^{-6} mm^3/ (N·m).[17−24]

The ultralow wear behavior of these composites is associated with the formation of a thin, robust tribofilm on both sliding surfaces.[20,22,25,26] The mechanism for the formation of these films has yet to be fully described. In fact, some debate exists as to whether the formation of the film is necessary to maintain the ultralow wear of the PTFE/alumina system, or whether it is simply a consequence of the wear debris morphology of the composite. Recent publications have maintained that the effect of the countersurface on low wear is purely mechanical, and the surface chemistry is not a significant factor in the formation of the transfer film.[27] Others have proposed structures[28,29] and performed computational modeling[30−32] in an attempt to describe the formation of new chemical species at the interface, but a clear understanding of the formation of new reactive end groups and how they interact with the metal surface and the filler has not previously been described.

Chemical analyses of PTFE/alumina transfer films in various stages of development, made possible by a "stripe test",[23,24,33] led to a proposed chemical mechanism responsible for the exceptional wear performance of these PTFE/α-alumina composites. The ultralow wear mechanism involves the breaking of PTFE carbon−carbon bonds at the interface. This chain scission occurs even at ambient temperatures, and at relatively low speeds and pressures. The next chemical reactions require oxygen and water from the ambient environment to produce reactive polymer end groups. The recirculation of wear debris eventually leads to thin, robust, and adherent polymeric transfer and running films which protect both the metal surface and the polymer from wear. Upon establishing thin and robust tribofilms the wear of the PTFE/alumina composites falls into the range of 10^{-7} to 10^{-8} mm^3/(N·m). A deeper understanding of the ultralow wear mechanisms for these exceptional materials could lead to new applications and new design paradigms.

2. MATERIALS AND METHODS

2.1. Tribology Test Methods. A "stripe test"[23,24,33] was performed in which the reciprocating stroke length decreased as the number of sliding cycles increased at predetermined cycle intervals (Figure 1a). This pattern of transfer film formation preserved and isolated lower cycle areas of the polymeric film on the metal. These areas acted as snapshots, allowing physical and chemical analyses of the steps involved in transfer film evolution.

The stripe test was performed using a linear reciprocating tribometer with flat-on-flat sample geometry as described by Schmitz.[34] A six-axis force transducer measured normal and frictional forces. The polished face of the polymer sample was loaded against the stainless steel countersample at 250 N for a nominal contact pressure of around 6.3 MPa. The contact pressure may be approximated in this way given that the polymer sample wears into conformity with the surface within the first thousand cycles. Initial asperities under much higher contact pressure are quickly worn away. The steel countersample reciprocated at 50.8 mm/s on a linear ball-screw stage. The reciprocating stroke length started at 88.9 mm and was reduced by 10.2 mm after each experiment until the final test which was 27.9 mm long.

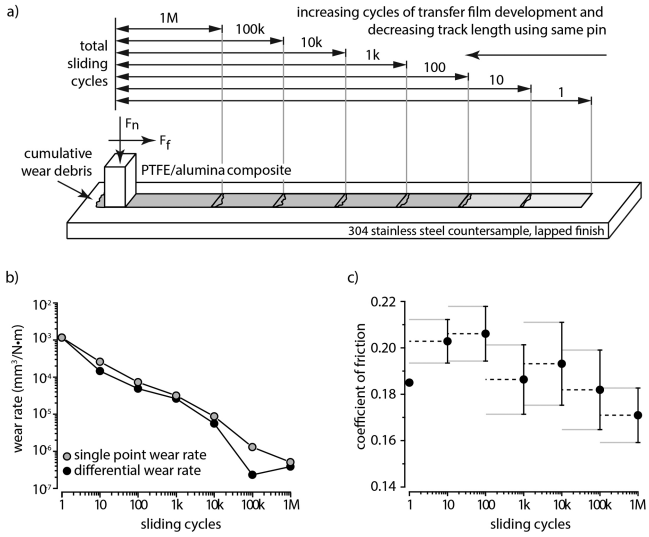

Figure 1. (a) A stripe test utilized spatial intervals in sliding to expose the stages of transfer film and wear debris evolution from one to one million cycles. (b) Single point and differential wear rates of the composite decrease as sliding progresses. (c) The friction coefficient of the composite decreases as sliding progresses. Error bars indicate the standard deviation of the measurement during each test, dotted lines span the duration of the tests over which averages were measured. Reprinted with permission from ref 23. Copyright 2015 Springer.

2.2. Measurements of Friction. Friction coefficients were calculated as the quotient of the average frictional force and the average normal force.[34] The associated uncertainties in the friction coefficient and wear rate calculations are described in greater detail in Schmitz et al.[34,35]

2.3. Measurements of Wear. The change in mass of the polymer sample after each test, m_{loss}, was measured using a Mettler Toledo scale (±10 μg) and was used in conjunction with the density of the sample, ρ, to calculate the change in volume per test, V_{loss}. This wear volume, V_{loss} (mm^3), divided by the product of the normal force, F_n (N), and the sliding distance, d (m), produces a wear rate, K, as described by Archard,[36] reported in units of mm^3/(N·m) (eq 1). Wear rates are commonly calculated both as total volume lost per total distance slid (single point wear rate), and as volume lost per test per distance slid per test (differential wear rate), Figure 1b. The total wear rate therefore includes the run-in period of relatively high wear before the onset of ultralow wear upon the stabilization of the transfer and running films on the steel countersurface and the polymer sliding surface, respectively. The test wear rate conveniently differentiates between early, higher wear rates, and the ultralow minimums reached at a high number of sliding cycles. A "steady state" wear rate is defined as the wear rate reached and maintained after the run-in period.

$$K = \frac{m_{loss}}{\rho F_n d} = \frac{V_{loss}}{F_n d} \quad (1)$$

2.4. Polymer Sample Preparation. A polymer composite was made using a DuPont Teflon PTFE 7C resin matrix filled with 5 wt % α-phase alumina (Nanostructured & Amorphous Materials Inc., Stock No. 1015WW).[21,23,37,38] The polymer sample was molded and prepared as previously described in Pitenis et al.,[23] sonicated in methanol for 30 min, and allowed to dry for 3 h in laboratory air prior to testing.

The powder mixture was sonicated in extra dry 2-propanol using an ultrasonic horn and placed in a fume hood where the solvent was

DOI: 10.1021/acs.macromol.5b00452
Macromolecules XXXX, XXX, XXX−XXX

allowed to evaporate. The dried powder mixture was compressed in a 440C stainless steel cylindrical mold to approximately 100 MPa in a hydraulic press. The sample was sintered in an oven, ramped at 2 °C/min to 380 °C, where it was held for 4 h and then cooled to room temperature. It was then machined into a pin (6.3 × 6.3 × 12.7 mm). The square faces of the pin were polished with 800 grit silicon carbide sandpaper to an approximate average roughness (Ra) of 100 nm.

2.5. Metal Countersurface Sample and Preparation. The countersample used in this experiment was a flat, rectangular (115 × 25 × 3.7 mm) plate of 304 stainless steel finished with a lapping process (Ra ~ 150 nm), the standard running surface used in previous experiments with the PTFE/alumina composites.[19,21,23,25,26,39] The countersample was cleaned with soap and water, rinsed with methanol, and allowed to dry for approximately 20 min prior to experiments.

2.6. Spectroscopy. Infrared spectra used to analyze the worn metal surfaces and transfer films were obtained using a Thermo Scientific Nicolet 6700 FT-IR spectrometer with a Thermo Scientific Nicolet Continuμm infrared microscope (Thermo Fisher Scientific) in reflectance mode. A 100 μm square aperture defined the area of analysis. Background spectra were collected in a clean area on the metal, away from the fluoropolymer wear track.

Transfer film spectra were obtained by reflectance off of the midpoint of the worn metal surface at three spots along the centerline within each of the seven exposed transfer film areas using an FT-IR microscope with a 100 μm aperture. This triplicate analysis showed consistent results within a given exposed area.

The cumulative wear debris from the edge of the 1 M cycles region was analyzed by attenuated total reflectance infrared (ATR-IR) using a Golden Gate (Specac) horizontal diamond ATR unit. Polymer spectra were collected with pressure applied from the overhead clamping device. Spectra were corrected for the ATR effect (depth of penetration versus wavenumber) to closely resemble transmission spectra. Transfer residue spectra were collected after polymer samples were analyzed and removed from the diamond surface, but before cleaning with ethanol. No pressure was applied from the clamping device for residue spectra. Background spectra were collected with a clean diamond surface.

Transmission spectra of the pressed polymer films (PTFE 7C/α-alumina/$C_6F_{13}COOH$ and PTFE 7C/α-alumina) were obtained using a Nicolet Magna 560 FT-IR spectrometer (Thermo Fisher Scientific). A background spectrum was first collected with an empty film card of the type used to mount the films. Spectra were converted to absorbance for comparison, and the end group region (1300−1800 cm^{-1}) was examined. The most effective means to detect changes in this region was to use a C−F overtone peak near 2365 cm^{-1} as a guide (after spectral subtraction of a PTFE 7C control film). The region below ~1320 cm^{-1} was distorted due to the intense C−F stretch region of these thick disk samples.

3. RESULTS AND DISCUSSION

The wear and friction performance of the PTFE/α-alumina composite was consistent with previous studies of similar composite materials.[19−23,27,40] Over the first 10k cycles a run-in period of moderately high wear was observed, followed by a decrease in wear rate over the next 100k cycles to less than 10^{-6} $mm^3/(N{\cdot}m)$ (Figure 1b). The coefficient of friction also decreased slightly over the course of the experiment (Figure 1c), remaining near $\mu \sim 0.19$.

Fourier transform infrared spectroscopy (FT-IR) was performed within the exposed areas of transfer film formed during the 1, 100k, and 1M cycle tests and on the cumulative wear debris for chemical analysis of the evolution of the wear system. FTIR analysis of the 1 cycle transfer film verified that fluoropolymer had been transferred to the metal, yet revealed an unusual set of peaks in the C−F region consisting of the typical PTFE peaks at 1203 and 1149 cm^{-1} along with a new peak at 1253 cm^{-1} (Figure 2a). This additional peak, originally

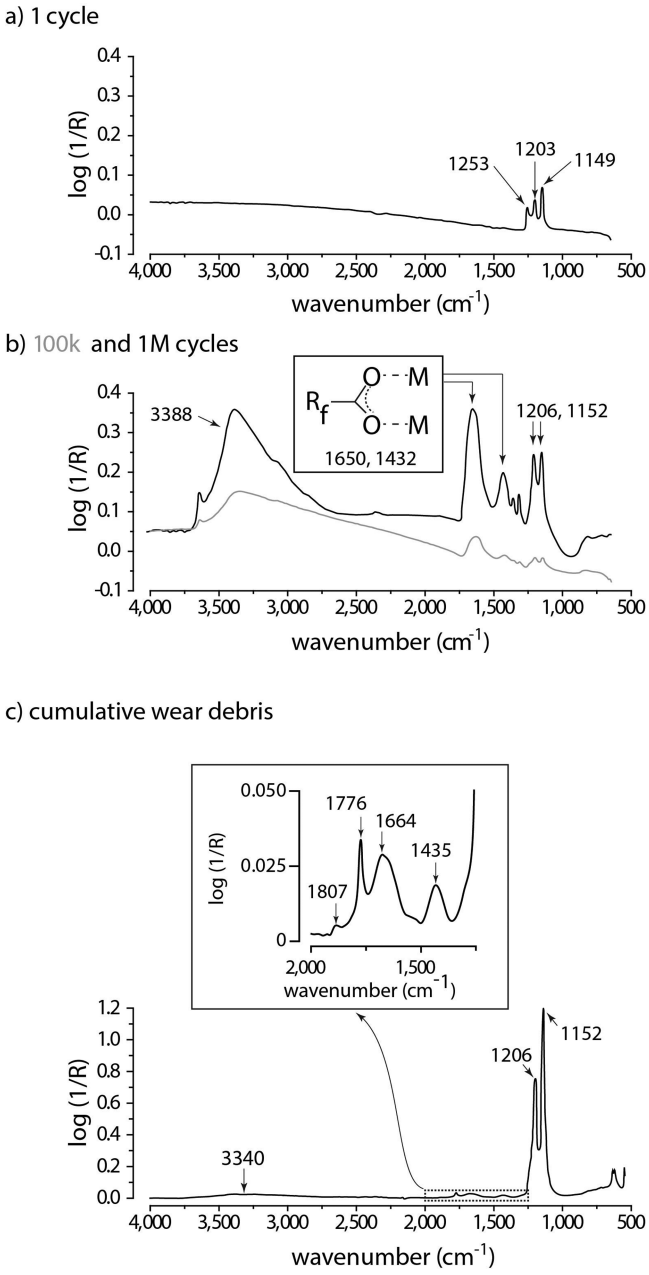

Figure 2. Infrared reflectance results from the metal surface after (a) one cycle of sliding, (b) 100k (gray line) and 1M (black line) cycles, and (c) ATR-IR spectrum of cumulative wear debris. Reprinted with permission from ref 23. Copyright 2015 Springer.

derived from first-principles calculations by Moynihan in 1959[41] has rarely been observed experimentally. To our knowledge, it has previously been observed for PTFE powder/film,[42] PTFE polymer slid against a film of polyethylene,[43] and PTFE polymer slid against 304 stainless steel.[44] Lauer attributed variations in intensity of the peak near 1250 cm^{-1} to a stretching mode of the polymer molecule, and noted that its intensity varied with respect to the alignment of helical PTFE chains relative to the detector when using a polarizer.[44] This observation implied that aligned PTFE chains were transferred to steel after a single sliding pass, which agrees with surface plasmon resonance results from Krick et al.[45] and XPS results from Uçar.[46]

DOI: 10.1021/acs.macromol.5b00452
Macromolecules XXXX, XXX, XXX−XXX

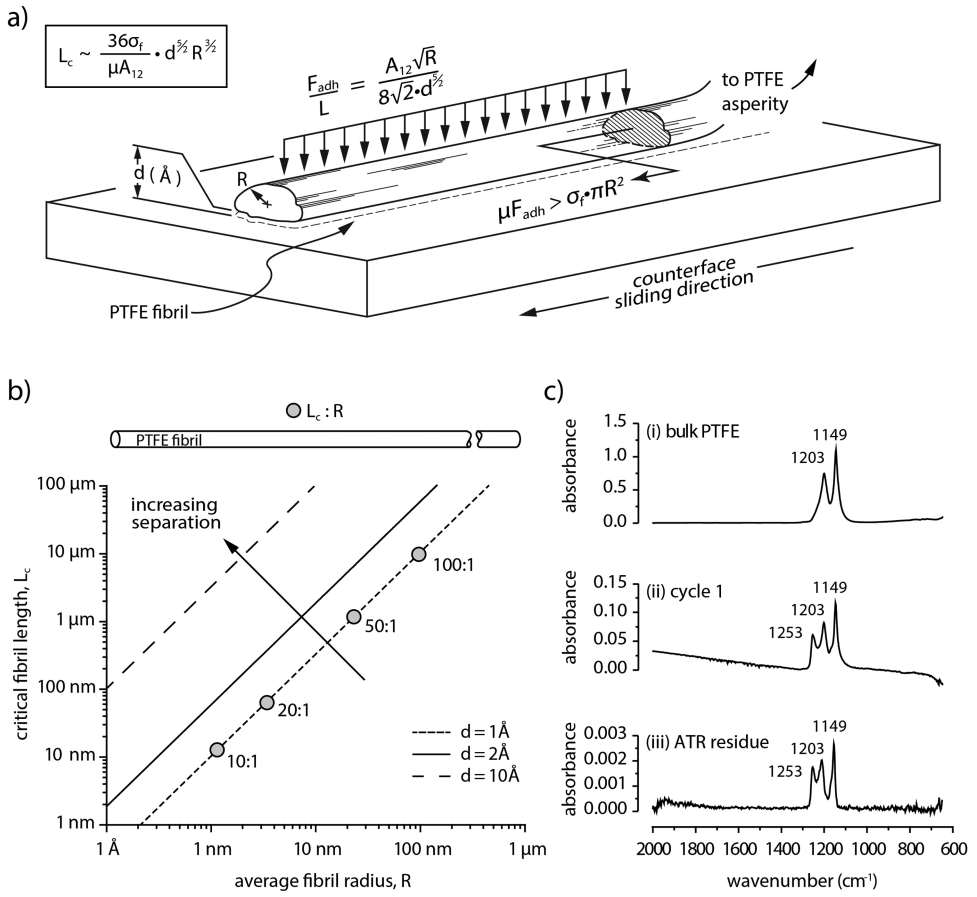

Figure 3. (a) PTFE filament of average radius R at separation distance d from a countersample must be in contact over a length L_c in order to break under tension imposed during sliding. (b) Plot of critical fibril length L_c versus average fibril radius R for separation d = 1, 2, and 10 Å illustrates the increase in L_c as R and d increase. The shaded circles represent aspect ratios as indicated. (c) (i) IR spectra of bulk PTFE, (ii) the 1 cycle transfer film, and (iii) the residue on the ATR crystal after pulling away from the bulk.

Because of its extremely high molecular weight (~ tens of millions g/mol[47]), granular PTFE is unlikely to transfer an entire chain to the metal surface, thus C−C backbone bond scission is likely involved. A simple mathematical argument can be made to support the bond breaking and transfer of PTFE chains in the first cycle of sliding. The model is based on a balance between the sum of all the van der Waals attractions between a PTFE fibril aligned to the sliding direction (as has been observed historically[8,13,48−51]) and the metal surface, and the force required to break a PTFE fibril (Figure 3). In the case of expanded PTFE in which PTFE filaments are highly aligned, the tensile strength of the fibril is approximately 400−700 MPa. The Hamaker solution for the attractive energy between a flat surface and a cylinder is a function of the Hamaker constant, A_{12} (here, the theoretical value of the Hamaker constant for PTFE-silica (7.6×10^{-20} J) was used[52]), the radius of the fibril, R, the length of the fibril, L, and the separation distance between the fibril and the surface, d. The energy equation may be differentiated to yield the attractive force, F_{adh}, per unit length (eq 2). Multiplying the attractive force, F_{adh}, by the friction coefficient of PTFE (~0.1) yields the force applied to an aligned fibril in contact over the length, L during sliding. Setting this force equal to the force required to break the fibril, σ_f, eq 3 allows us to solve for a critical fibril length L_c (eq 4). Any fibril in contact with the countersurface over a length L_c or greater may be broken in sliding. This hypothesis is supported in the literature by Makinson in 1964[5] and Brainard in 1973,[53] and evidence for the transfer of oriented films of PTFE onto a glass substrate during sliding contact has previously been published.[54]

$$\frac{F_{adh}}{L} = \frac{A_{12}\sqrt{R}}{8\sqrt{2} \times d^{5/2}} \quad (2)$$

$$\mu F_{adh} = \sigma_f \pi R^2 \quad (3)$$

$$L_c \sim \frac{36\sigma_f}{\mu A_{12}} d^{5/2} R^{3/2} \quad (4)$$

A control spectrum of PTFE was obtained by slicing through the sample using a razor blade, thereby exposing the internal PTFE composite with no sliding history, but the same thermal and environmental history. When the diamond ATR crystal was held in place against this fresh surface, the spectrum contained the expected IR peaks observed for bulk PTFE (Figure 3c-i) at 1203 and 1149 cm^{-1}. After the diamond ATR crystal was removed from contact with the bulk PTFE, the IR spectrum was reacquired in air. Not only were peaks in the C−F region still visible, but the spectrum now included an additional absorbance peak at 1253 cm^{-1} (Figure 3c-iii), giving a spectrum identical to the one from the 1 cycle sliding experiment (Figure 3c-ii). This is evidence for the transfer of aligned PTFE chains from the cut surface of the composite to the ATR crystal after simple static contact. The same trio of infrared peaks was also

DOI: 10.1021/acs.macromol.5b00452
Macromolecules XXXX, XXX, XXX−XXX

obtained from similar polymer transfer to the ATR crystal under static contact from an as-molded PTFE surface, which eliminated the razor cut as the source of the transferred polymer chains. Transfer of PTFE to metal surfaces through static contact in high vacuum has also been observed by Auger photoelectron spectroscopy (AES),[53] but to our knowledge this has never been observed in ambient air.

Within the 100k cycle region new broad peaks at 3388, 1650, and 1432 cm^{-1} were observed, in addition to the PTFE backbone peaks at 1203 and 1149 cm^{-1}, and within the 1 M cycle region these peaks dominate the spectrum (Figure 2b). In perfluoropolymers, carboxylic acid end groups[55] are often observed. The peaks are relatively sharp and are assigned to a mixture of both monomer (1775 cm^{-1}) and dimer (1813 cm^{-1}) forms. Much broader and lower frequency carbonyl peaks (1655, 1441 cm^{-1}) have been reported for fluorinated carboxylic acids chelated to metals as shown by Kajdas et al.[56,57] In Kajdas' experiment, perfluorooctanoic acid ($C_7F_{15}COOH$) was coated onto a steel surface and then heated, and the resulting spectrum is reproduced in Figure 4a.

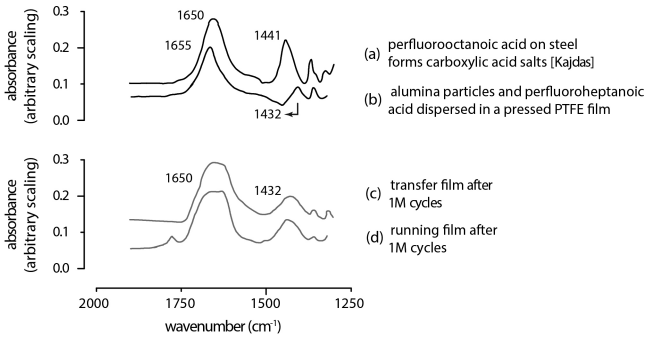

Figure 4. IR carbonyl-region spectra of the transfer film and running film compared to small molecule model reactions with perfluorinated carboxylic acids: (a) IR spectrum from Kajdas and Przedlacki[57] (used with permission) showing the chelated salt of perfluorooctanoic acid on a steel surface; (b) IR spectrum obtained from a PTFE film filled with a mixture of alumina particles and perfluoroheptanoic acid; (c) IR reflectance spectrum of the 1 M cycle transfer film on the metal; (d) ATR-IR spectrum of the running surface of the polymer pin after 1 M cycles.

Figure 4c shows the striking similarity between the data from Kajdas and the IR spectrum taken from the 1 M cycle region, indicating similar metal chelation must occur in each case. Note that the peak at 1655 cm^{-1} also contains an absorbance for water, with other water peaks appearing above 3000 cm^{-1}.

In a separate experiment, a small molecule model compound ($C_6F_{13}COOH$) and the same α-alumina were premixed and dispersed in PTFE 7C. The result was a transmission IR spectrum (Figure 4b) also very similar to that of the ATR-IR spectrum of the running film (Figure 4d). Additionally, the ATR-IR spectrum of the running surface of the polymer was quite similar to that of the transfer film, indicating similar chemical changes in each. A control experiment without α-alumina yielded the expected much sharper monomer and dimer R_f−COOH acid peaks at 1813 and 1775 cm^{-1}, respectively. These IR results suggest that PTFE carboxylate chain ends not only chelate to the steel surface under the transfer film, but also to the surface of the alumina filler particles. Hydrocarbon carboxylic acids are known to react with the amphoteric surface of alumina particles,[58] so it is not surprising that perfluorinated carboxylic acids, which are much stronger Brønsted acids,[59] react with and chelate to the alumina surface, even in the absence of heating.

The sample for Figure 4b was made by combining α-alumina from the same source as used for the composite (10 g), tridecafluoroheptanoic acid ($C_6F_{13}COOH$, TCI America, 98%, 0.23 g) and dry isopropyl alcohol (99.9%, 0.010% water, 30 mL) in a drybox. The α-alumina had been predried in a Schenk flask in a 150 °C oil bath for 5 h, which was then backfilled with dry nitrogen and sealed for transportation to the drybox. (Isopropyl alcohol was chosen since it could disperse the alumina and dissolve the acid.) The slurry was stirred briefly in the drybox, moved into the fume hood, then reduced *in vacuo* (150 Torr) in a 29 °C water bath to minimize vaporization of the acid. Using a roller mill, the acid/alumina mixture (0.53 g) was dispersed in dried PTFE 7C (10 g) over 18 h. A control sample for IR comparison to the PTFE 7C/α-alumina/acid mixture was created in a drybox by dissolving tridecafluoroheptanoic acid (11 mg) in Freon-11 (trichlorofluoromethane, 99%), which was then added to PTFE 7C, predried in the same manner as previously described. The solvent was removed in a water bath *in vacuo* as previously described.

These polymer mixtures were prepared for IR analysis by cold pressing into 13 mm circular disks approximately 100 mg each. Duplicate samples were prepared under 2.5−3 tons of force in a hydraulic press at ambient temperature. Pressing resulted in films approximately 350 μm thick.

ATR-IR analysis (Figure 2c) of the cumulative wear debris at the end of the 1 M cycle track (shown schematically in Figure 1a) showed large absorbance peaks for the PTFE backbone, but also contained smaller peaks for monomer and dimer carboxylic acids as well as the chelated salts. The cumulative wear debris contained polymer fragments shed during the entire wear process. As such, the chain-end chemical intermediates were observed here because further chemical modification or chelation was not possible after ejection from the wear track.

The analysis of the evolution of the transfer film made possible by the design of the stripe test, combined with years of laboratory wear test observations, led to the chemical mechanism proposed in Figure 5. Parts a and b of Figure 5 illustrate the first step of the process: mechanochemical breaking of a PTFE carbon−carbon bond[5,53] to form perfluoroalkyl radicals. The steps of Figure 5b−e are mechanistically identical to e-beam irradiation of high molecular weight PTFE in ambient air.[60−62] The perfluoroalkyl radicals react with atmospheric oxygen to form a peroxy radical (Figure 5c), which further decomposes into the more stable acyl fluoride end group (Figure 5d). The acyl fluoride end group is unstable toward water and will therefore hydrolyze in ambient humidity to form a carboxylic acid (Figure 5e). The dependence of the wear rate of this system on humidity and vacuum environments has been described previously.[19,21] The HF produced[55] during these steps likely goes on to form metal fluorides at the surface of the countersample. The carboxylic acids are able to chelate to the steel countersurface (Figure 5f), strongly adhering them to the surface to form the thin and robust transfer film.[20,37]

Jintang and Hongxin[28] present a similar mechanism for mechanochemistry of PTFE, but do not mention the critical carboxylate groups which are the cause of the adhesive interaction between the transfer film and the metal countersurface. Furthermore, the chelation of −COOH ended PTFE chains to the alumina fillers at the interface further reinforces

DOI: 10.1021/acs.macromol.5b00452
Macromolecules XXXX, XXX, XXX−XXX

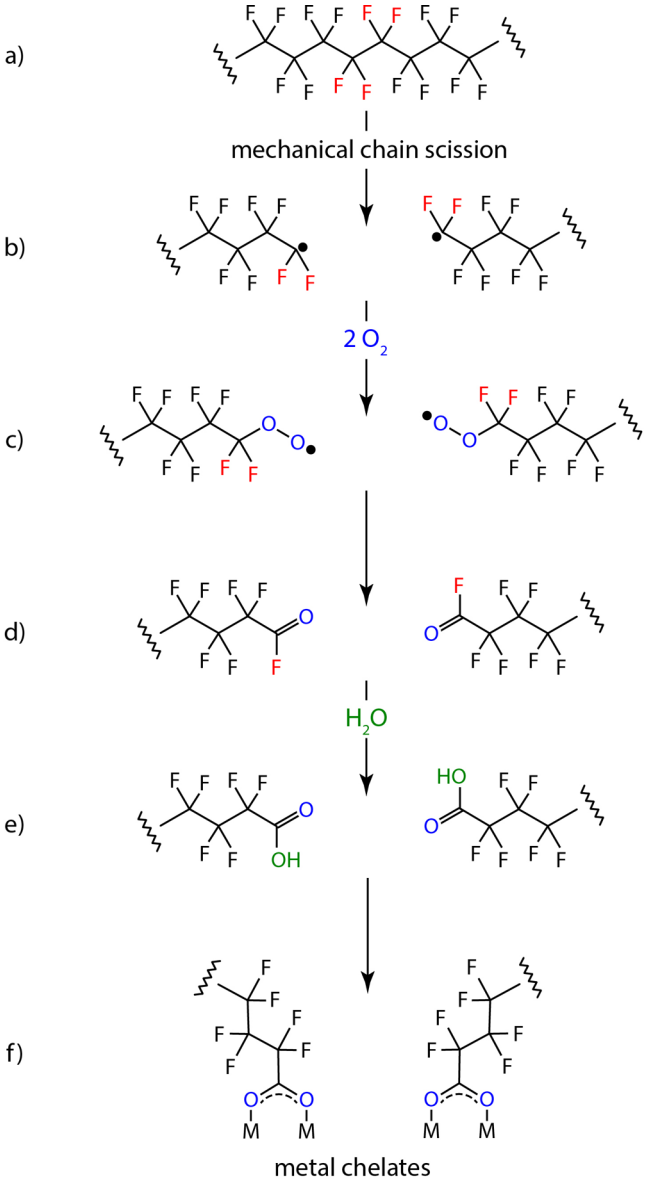

Figure 5. Chain scission of PTFE (a) is caused mechanically by sliding (b). Environmental oxygen reacts with the radicals at the broken chain ends (c). These unstable end groups decompose to form an acyl fluoride (d). Moisture in the air hydrolyzes these groups to make carboxylic acids (e). Carboxylic acid end groups react with and chelate to the surface of the metal and alumina particles (f).

the running surface of the polymer, which in turn reduces the wear rate and the creep of the system. The mechanochemical interaction between the PTFE/α-alumina composite is the first step in a complex cascade of events. Low wear in this instance is a property of the system created during sliding, and as previously mentioned it is heavily dependent on the environment. Despite much milder conditions than what are typically required for thermal bond cleavage in PTFE,[63] similar reaction products are nonetheless detected in both the running and transfer films at the interface (Figure 6). At low sliding speeds, low nominal contact pressure, and a deviation not more than ~1 °C from ambient temperature, it is the coupling of mechanical and chemical effects that ultimately facilitates the formation of the transfer and running films necessary to

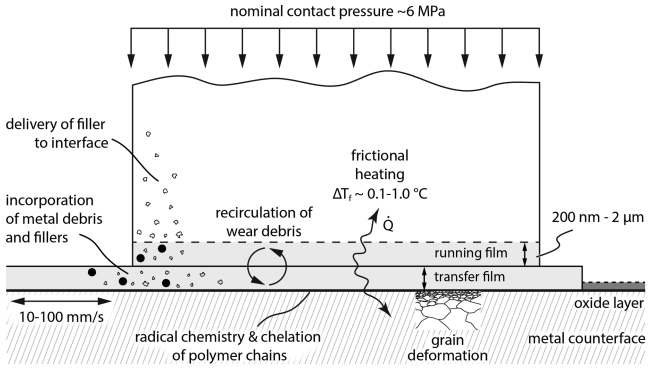

Figure 6. Low wearing tribological system is complex and subject to numerous variables. Radical chemistry at the sliding interface proceeds despite low speed, low nominal contact pressure, and low frictional temperature change. The circulation, rather than ejection, of debris between the transfer and running films is key to the high cycle maintenance of ultralow wear.

maintain low wear for hundreds of thousands to millions of sliding cycles.

4. CONCLUSIONS

Transfer of PTFE to the metal countersurface occurs during the first cycle of sliding as evidenced by FT-IR (Figure 2a) via mechanochemical chain scission supported by a van der Waals model given in Figure 3. As described previously, the wear rate of the composite was high during the run-in period and did not fall below 10^{-6} mm^3/(N·m) until the 100k cycle test. This coincided with the appearance of IR peaks at 1650 and 1432 cm^{-1} (Figure 2b, Figure 4, parts c and d) which indicated the presence of chelated carboxylate polymer chain ends in the transfer and running films (Figure 5f). The concentration of these species increased significantly during the 1M cycle test (Figure 2b) as more and more chains broke and reacted to form carboxylate chelates with either metal or Al_2O_3 surfaces. Carboxylic acid chain ends that were not able to chelate to the surface before being ejected as wear debris were the source of the carboxylic acid monomers and dimers seen by IR in the cumulative wear debris (Figure 2c).

The formation of an ultralow wear PTFE transfer film on 304 stainless steel is a complex process that involves the chemical interaction between the polymer composite, the embedded alumina particles, the ambient atmosphere, and the metal countersurface. Under reciprocating testing conditions, this is a cycle-dependent process relying on the mechanical input of energy to cause chain scission which initiates the radical-driven mechanism of transfer film formation. The individual reactions proposed have been previously observed in nontribological settings, but put together in this context they provide chemical insight into the observed wear behavior of this filled-PTFE composite. As illustrated in Figure 6, the formation and maintenance of this ultralow wear system arises from a complex set of variables which allow for the chemical modification of both sliding surfaces under relatively mild conditions.

AUTHOR INFORMATION

Corresponding Author

*(C.P.J.) Telephone: (302) 695-4550. E-mail: Christopher.P.Junk@DuPont.com.

Notes

The authors declare no competing financial interest.

DOI: 10.1021/acs.macromol.5b00452
Macromolecules XXXX, XXX, XXX−XXX

■ ACKNOWLEDGMENTS

The authors thank the following people for support and helpful technical conversations: Heidi Burch, David L. Burris, Gary Halliday, Timothy Krizan, and Neil Washburn.

■ REFERENCES

(1) Renfrew, M. M.; Lewis, E. E. *Ind. Eng. Chem.* **1946**, *38* (9), 870−877.
(2) Shooter, K. V.; Tabor, D. *Proc. Phys. Soc., Sect. B* **1952**, *65* (9), 661−671.
(3) King, R. F.; Tabor, D. *Proc. Phys. Soc., Sect. B* **1953**, *66* (9), 728−736.
(4) Flom, D. G.; Porile, N. T. *J. Appl. Phys.* **1955**, *26* (9), 1088.
(5) Makinson, K. R.; Tabor, D. *Proc. R. Soc. London, Part A: Math. Phys. Eng. Sci.* **1964**, *281* (1384), 49−61.
(6) Blanchet, T. A.; Kennedy, F. E. *Wear* **1992**, *153* (1), 229−243.
(7) Gong, D.; Xue, Q.; Wang, H. *Wear* **1989**, *134*, 283−295.
(8) Tanaka, K.; Uchiyama, Y.; Toyooka, S. *Wear* **1973**, *23* (2), 153−172.
(9) Tanaka, K.; Kawakami, S. *Wear* **1982**, *79* (2), 221−234.
(10) Blanchet, T. A.; Kennedy, F. E.; Jayne, D. T. 1993.
(11) De-Li, G.; Bing, Z.; Qun-Ji, X.; Hong-Li, W. *Wear* **1990**, *137* (2), 267−273.
(12) Lai, S.-Q.; Yue, L.; Li, T.-S.; Hu, Z.-M. *Wear* **2006**, *260* (4−5), 462−468.
(13) Wheele, D. R. The transfer of polytetrafluoroethylene studied by X-ray photoelectron spectroscopy. *Wear* **1981**, *66*, 355−365.
(14) Fischer, D.; Lappan, U.; Hopfe, I.; Eichhorn, K.; Lunkwitz, K. *Polymer* **1998**, *39* (3), 573−582.
(15) Yuan, X.-D.; Yang, X.-J. *Wear* **2010**, *269* (3−4), 291−297.
(16) Shi, Y. J.; Feng, X.; Wang, H. Y.; Liu, C.; Lu, X. H. *Tribol. Int.* **2007**, *40* (7), 1195−1203.
(17) Li, F.; Hu, K.; Li, J.; Zhao, B. *Wear* **2001**, *249* (10−11), 877−882.
(18) Burris, D. L.; Sawyer, W. G. *Wear* **2006**, *260* (7), 915−918.
(19) Krick, B. A.; Ewin, J. J.; Blackman, G. S.; Junk, C. P.; Sawyer, W. G. *Tribol. Int.* **2012**, *51*, 42−46.
(20) Ye, J.; Khare, H. S.; Burris, D. L. *Wear* **2014**, *316* (1−2), 133−143.
(21) Pitenis, A. A.; Ewin, J. J.; Harris, K. L.; Sawyer, W. G.; Krick, B. A. *Tribol. Lett.* **2014**, *53* (1), 189−197.
(22) Krick, B. A.; Ewin, J. J.; McCumiskey, E. J. *Tribol. Trans.* **2014**, *57* (6), 1058−1065.
(23) Pitenis, A. A.; Harris, K. L.; Junk, C. P.; Blackman, G. S.; Sawyer, W. G.; Krick, B. A. *Tribol. Lett.* **2015**, *57* (1), 4.
(24) Urueña, J. M.; Pitenis, A. A.; Harris, K. L.; Sawyer, W. G. *Tribol. Lett.* **2015**, *57* (1), 9.
(25) Burris, D. L.; Sawyer, W. G. *Tribol. Trans.* **2005**, *48* (2), 147−153.
(26) Burris, D. L.; Zhao, S.; Duncan, R.; Lowitz, J.; Perry, S. S.; Schadler, L. S.; Sawyer, W. G. *Wear* **2009**, *267* (1−4), 653−660.
(27) Blanchet, T.; Kandanur, S.; Schadler, L. *Tribol. Lett.* **2010**, *40* (1), 11−21.
(28) Jintang, G.; Hongxin, D. *J. Appl. Polym. Sci.* **1988**, *36* (1), 73−85.
(29) Aderikha, V. N.; Krasnov, A. P.; Shapovalov, V. A.; Golub, A. S. *Wear* **2014**, *320*, 135−142.
(30) Zuo, Z.; Yang, Y.; Qi, X.; Su, W.; Yang, X. *Wear* **2014**, *320*, 87−93.
(31) Onodera, T.; Kawasaki, K.; Nakakawaji, T.; Higuchi, Y.; Ozawa, N.; Kurihara, K.; Kubo, M. *J. Phys. Chem. C* **2014**, *118*, 11820−11826.
(32) Onodera, T.; Park, M.; Souma, K.; Ozawa, N.; Kubo, M. *J. Phys. Chem. C* **2013**, *117*, 10464−10472.
(33) Wahl, K. J.; Singer, I. L. *The Third Body Concept Interpretation of Tribological Phenomena*; Tribology Series; Elsevier: Amsterdam, 1996; Vol. *31*.
(34) Schmitz, T. L.; Action, J. E.; Ziegert, J. C.; Sawyer, W. G. *J. Tribol.* **2005**, *127*, 673.
(35) Schmitz, T. L.; Action, J. E.; Burris, D. L.; Ziegert, J. C.; Sawyer, W. G. *J. Tribol.* **2004**, *126* (4), 802.
(36) Archard, J. F. *J. Appl. Phys.* **1953**, *24* (8), 981.
(37) Ye, J.; Khare, H. S.; Burris, D. L. *Wear* **2013**, *297* (1−2), 1095−1102.
(38) Junk, C. P.; Sawyer, W. G.; Krick, B. A.; Blackman, G. S.; Wetzel, M. D. Low-Wear Fluoropolymer Composites, World Patent Application WO2012158650A1 (2012).
(39) Burris, D. L.; Perry, S. S.; Sawyer, W. G. *Tribol. Lett.* **2007**, *27* (3), 323−328.
(40) Sawyer, W. G.; Argibay, N.; Burris, D. L.; Krick, B. a. *Annu. Rev. Mater. Res.* **2014**, *44* (1), 395−427.
(41) Moynihan, R. E. *J. Am. Chem. Soc.* **1959**, *81* (5), 1045−1050.
(42) Zerbi, G.; Sacchi, M. *Macromolecules* **1973**, *6* (5), 692−699.
(43) Jain, V. K.; Bahadur, S. *Wear* **1978**, *46* (1), 177−188.
(44) Lauer, J. L.; Bunting, B. G.; Jones, W. R. *Tribol. Trans.* **1988**, *31* (2), 282−288.
(45) Krick, B. A.; Hahn, D. W.; Sawyer, W. G. *Tribol. Lett.* **2012**, *49* (1), 95−102.
(46) Uçar, A.; Çopuroğlu, M.; Baykara, M. Z.; Arıkan, O.; Suzer, S. *J. Chem. Phys.* **2014**, *141* (16), 164702.
(47) Kricheldorf, H.; Nuyken, O.; Swift, G. *Handbook of Polymer Synthesis*; Marcel Dekker: New York, 2004
(48) Breiby, D. W.; Sølling, T. I.; Bunk, O.; Nyberg, B.; Norrman, K.; Nielsen, M. M. 2005, 2383−2390.
(49) Jang, I.; Burris, D. L.; Dickrell, P. L.; Barry, P. R.; Santos, C.; Perry, S. S.; Phillpot, S. R.; Sinnott, S. B.; Sawyer, W. G. *J. Appl. Phys.* **2007**, *102* (12), 123509.
(50) Beamson, G.; Clark, D. T.; Deegan, D. E.; Hayes, N. W.; S.-L. Law, D.; Rasmusson, J. R.; Salaneck, W. R. *Surf. Interface Anal.* **1996**, *24* (3), 204−210.
(51) Wittmann, J. C.; Smith, P. *Nature* **1991**, *352* (6334), 414−417.
(52) Asencio, R. Á.; Cranston, E. D.; Atkin, R.; Rutland, M. W. *Langmuir* **2012**, *28* (26), 9967−9976.
(53) Brainard, W. A.; Buckley, D. H. *Wear* **1973**, *26* (1), 75−93.
(54) Fenwick, D.; Ihn, K. J.; Motamedi, F.; Wittmann, J.-C.; Smith, P. *J. Appl. Polym. Sci.* **1993**, *50* (7), 1151−1157.
(55) Pianca, M.; Barchiesi, E.; Esposto, G.; Radice, S. *J. Fluorine Chem.* **1999**, *95* (1−2), 71−84.
(56) Kajdas, C. K. *Tribol. Int.* **2005**, *38* (3), 337−353.
(57) Przedlacki, M.; Kajdas, C. *Tribol. Trans.* **2006**, *49*, 202−214.
(58) Luiz, N.; Filho, D. *Encycl. Surf. Colloid Sci.* **2004**, *1*, 209−228.
(59) Goss, K.-U. *Environ. Sci. Technol.* **2008**, *42* (2), 456−458.
(60) Fischer, D.; Lappan, U.; Hopfe, I.; Eichhorn, K.-J.; Lunkwitz, K. *Polymer (Guildf.).* **1998**, *39* (3), 573−582.
(61) Lappan, U.; Fuchs, B.; Geißler, U.; Scheler, U.; Lunkwitz, K. *Polymer* **2002**, *43*, 4325−4330.
(62) Dorschner, H.; Lappan, U.; Lunkwitz, K. *Nucl. Instruments Methods Phys. Res., Sect. B: Beam Interact. Mater. Atoms* **1998**, *139* (1−4), 495−501.
(63) Puts, G. J.; Crouse, P. L. *J. Fluorine Chem.* **2014**, *168*, 9−15.

DOI: 10.1021/acs.macromol.5b00452
Macromolecules XXXX, XXX, XXX−XXX